Indian Journal of Chemical Technology
Vol. 28, November 2021, pp. 735-739

Optimization of structural and optical properties of sputter deposited TiO_2 thin films by controlling deposition parameters

Prashant Yadav, Hitesh Kumar Sharma, Manohar Singh, Anil Kumar Malik & Beer Pal Singh*

Nanomaterials Laboratory, Department of Physics, CCS University, Meerut 250 004, Uttar Pradesh, India
E-mail: drbeerpal@gmail.com

Received 2 September 2021, accepted 30 September 2021

Titanium oxide (TiO_2) thin films have been deposited onto highly cleaned soda lime glass substrates by DC magnetron reactive sputtering system. The Ti target with purity 99.99% is sputtered by argon gas in the sputtering chamber. Oxygen gas with purity 99.99% is introduced during the deposition process into the sputtering chamber as reactive gas for the synthesis of titanium oxide. Structural and optical properties of TiO_2 thin films have been characterized by X-ray diffraction (XRD), Raman spectroscopy and UV-Vis. spectroscopy. The effect of substrate temperature and sputtering power on the optical properties of TiO_2 thin films has been studied. The XRD and Raman spectroscopy of as-deposited films are used to study the structural properties of TiO_2 as a function of substrate temperature and sputtered power. The structural studies show the crystalline nature of TiO_2 thin films. The narrowing of energy band gap of sputtered deposited TiO_2thin films was studied using UV-Vis. spectroscopy.

Keywords: Raman Spectroscopy, Thin Films, TiO_2, UV –Vis. Spectroscopy, XRD

Nowadays thin films of metal oxides (CuO, ZnO, SnO_2, TiO_2, V_2O_5 etc.) are largely used in different fields because they are transparent to the visible region and have high hardness. $TiO_2$is among the material fulfils all the required demands[1]. TiO_2 is non-toxic, low cost and chemical stable material. TiO_2 thin films have shows remarkable chemical, electrical and optical properties[2]. TiO_2 thin films structural and optical properties were widely investigated for their various applications like in solar cells[3], photocatalyst[4], antireflection coatings[5], water purifier[6], sensors[7] and self-cleaning[8]. Generally it found in three phases such as rutile, anatese and brookite. Rutile and anatase phase are generally used in photocatalysis. Rutile and anatase has various applications for industrial purpose.The band gap energy (Eg) of bulk TiO_2 lies ~3.36–3.43 eV and for the crystalline anatase and rutile phase is 3.2 and 3.0 eV, respectively[9].

TiO_2 thin films can be achieved by using various physical and chemical methods techniques like DC and RF magnetron sputtering[10], pulse laser deposition[11], electron beam evaporation[12], sol-gel method[13], dip coating[14], hydrothermal method[15] and spin coating[16]. Among these methods, magnetron sputtering technique have various advantages like good adhesion, less contamination, control deposition rates and can be performed at room temperature. The structural and optical properties of thin films are strictly depend on the preparation method, composition and the deposition parameters (film thickness, substrate temperature, sputtered power etc.)[17-22].

In present research work, we have achieved TiO_2 thin films by DC magnetron sputtering.We have studied the effect of sputtered power and substrate temperature on theTiO_2 thin films to improve its photo-response from UV to visible region[23]. Structural properties of TiO_2 thin films were determined from X-ray Diffractometer (XRD: Rigaku) with Cu-Kα_1 radiation of wavelength 1.54Å at the scanning rate 0.1 deg. per sec. The optical absorption spectra of TiO_2 thin films were measured at room temperature (Hitachi-U-3300 UV–Vis. Spectrophotometer). Raman spectra was analyzed (HR800 Horiba JobinYvon) with spectral resolution of ~ 1 cm^{-1}.

Experimental Section

Thin films of TiO_2 were deposited onto ultrasonically cleaned soda lime glass substrate by DC magnetron reactive sputtering system. The titanium target with 99.99% purity was used. The distance between the target and substrate was fixed at 6 cm. The Argon (Ar) and oxygen (O_2) gases with purity of 99.99% were used as sputtered and reactive gas respectively for the synthesis of TiO_2 thin films.

Sputtering process occurred in the chamber evacuated to the base pressure 9.5× 10^{-6} mbar and the sputtering pressure 2.5 × 10^{-2} mbar maintained during every sample deposition. The Ar and O_2 flow rate 20:4 (Ar:O_2) sccm and deposition time 10 minute is fixed for every sample preparation. The detailed process of TiO_2 thin films deposition shown in Fig. 1. Temperature and power were the parameters varied during the sample preparation, samples deposited at different sputtering power and substrate temperature named as P_1, P_2, P_3 and T_1, T_2, T_3 and T_4 respectively shown in Table 1 and Table 2.

Results and Discussion

X- Ray diffraction

Fig. 2(a) shows XRD patterns of the sputtered deposited TiO_2thin films at different sputter power. Weak intense peak and broadening of diffraction peaks for the different sputter power deposited thin films indicate the presence of amorphous phase. Amorphous nature of TiO_2 thin films disappear as the sputtered power increases from 100 W to 150 W and when further increase the sputtered power from 150W to 200 W the amorphous nature of TiO_2 thin films again dominate. The only sample P_2 shows the rutile phase (110) at 27.80º and the samples P_1 and P_3shows amorphous nature. If the distance between the substrate and the target is less, power is high. Then the collision is strong and the more energy transferred to the substrate and this decrease the chance to achieve the crystalline TiO_2 thin films. With the increase of distance between substrate and target and lower the sputter power it will increases the chances to achieve crystalline TiO_2thin films[24-29].

Fig. 2(b) shows the substrate temperature dependence of XRD patterns. At low substrate temperature, the surface mobility causes a less ordered surface crystal structure. The low mobility of

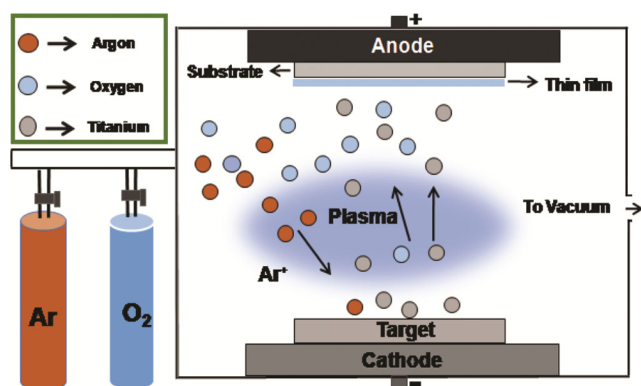

Fig. 1 — Schematic diagram of sputter deposited TiO_2 thin films.

Table1 — Deposition parameters for the synthesis of TiO_2thin films at various sputtered power.

Target	Gas used Ar:O_2 (sccm)	Substrate temperature (°C)	Sputtered power	Sample name
Ti	20:4	Room Temperature	100 Watt	P_1
Ti	20:4	Room Temperature	150 Watt	P_2
Ti	20:4	Room Temperature	200 Watt	P_3

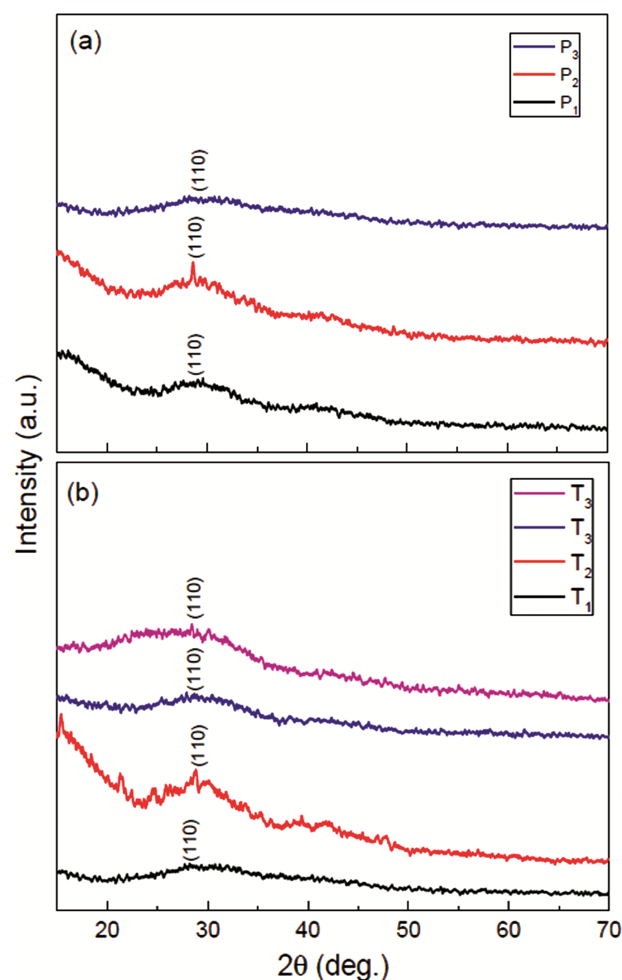

Fig. 2 — XRD pattern of TiO_2 thin films on glass substrates at: (a) various sputter power and (b) various substrate temperatures.

Table 2 — Deposition parameters for the synthesis of TiO_2thin films at various substrate temperatures.

Target	Gas used (sccm)	Substrate temperature (°C)	Sputtered power	Sample name
Ti	20:4	Room temperature	200 Watt	T_1
Ti	20:4	100	200 Watt	T_2
Ti	20:4	200	200 Watt	T_3
Ti	20:4	300	200 Watt	T_4

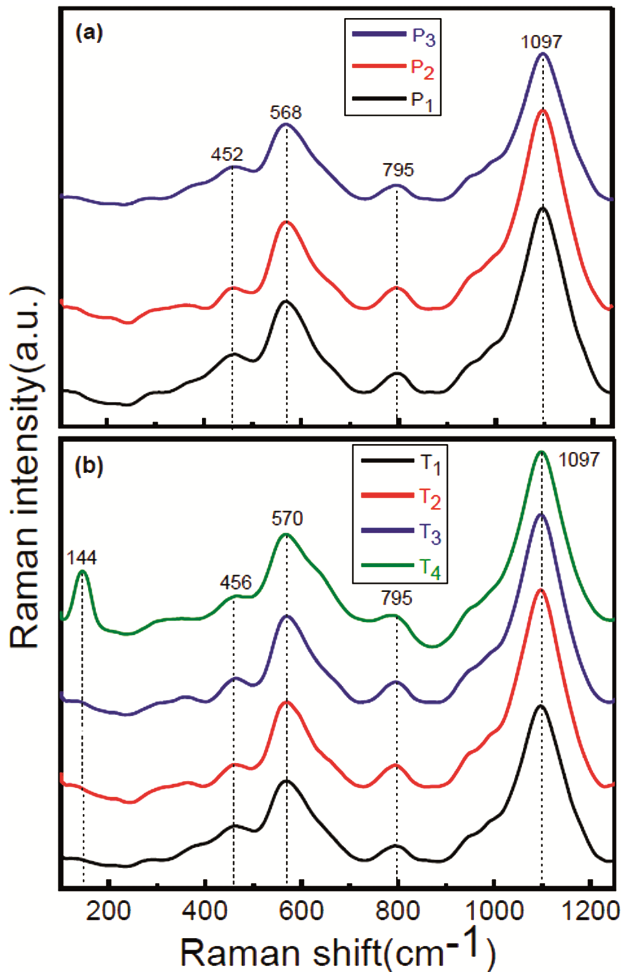

Fig. 3 — Raman spectra of TiO_2 thin films on glass substrates at: (a) various sputter power and (b) various substrate temperatures.

substrate atoms prevents full crystallization of the films. When we increase the substrate temperature, the substrate atoms achieve sufficient mobility to rearrange themselves in a more crystalline structure. XRD peak profile analysis revealed the rutile phase of TiO_2 thin films[30]. The sample T_2, T_3, and T_4 shows only one peak (110) at 27.8° for rutile phase. We can interoperate these results as the substrate temperature increases from room temperature to 300°C the TiO_2 thin film move amorphous to crystalline in nature.

Raman studies

Raman spectroscopy was used to determine the microstructure of sputtered deposit TiO_2 thin films and is an investigating tool to determine the vibrational and rotational structure. The Raman spectra of sputtered deposit TiO_2 thin films recorded in the range 200-1200 cm^{-1}.The rutile structure belong to the tetragonal space group D^{14}_{4h} ($P4_2/mnm$) and the anatase structure characterized to the tetragonal space group D^{19}_{4h} ($I4_1/amd$). The rutile and anatase have four and six Raman active modes respectively. Raman active modes for rutile are 143 cm^{-1} (B_1g), 447 cm^{-1} (E_g), 612 cm^{-1} (A_{1g}) and 826 (B_{2g}) cm^{-1}. The Raman active modes for anatase are 144 cm^{-1} (E_g) 197 cm^{-1} (E_g), 400 cm^{-1}(B_1g), 515 cm^{-1} (A_{1g}) and 519 cm^{-1}(B_1g) and 640 cm^{-1} (E_g). TiO_2 thin films Raman spectra deposited at different sputtered power are shown in Fig. 3(a).The Raman peaks at 452 cm^{-1} (E_g), 568 cm^{-1} (A_{1g}) and 795 (B_{2g}) cm^{-1} are the characteristic peak of rutile. Another intense peak observed at 1097cm^{-1} corresponds to vibrational mode. As the previous studies shows that the flow rate of argon and oxygen affects the crystallinity of sputtered deposited TiO_2 thin films. When flow rate of oxygen and argon is 1:2 sccm (O_2:Ar) or higher than this ratio the deposited TiO_2 thin films shows rutile structure only[29]. TiO_2 thin films Raman spectra deposited at different substrate temperature are shown in Fig. 3(b). The Raman peaks at 456 cm^{-1} (E_g), 570 cm^{-1} (A_{1g}) and 795 (B_{2g}) cm^{-1} are the characteristic peak of rutile. Another intense peak observed at 144 cm^{-1} (E_g) for sample T_4 is the characteristic peak of anatase. Another intense peak is also observed at 1097 cm^{-1} for vibrational mod[31-35].

UV-Vis Spectroscopy

Absorption spectra of sputtered deposit TiO_2thin films were recorded in the range 200-800 nm wavelength. The prepared thin films were transparent to visible light, these films are sensitive to UV light shorter than 375 nm wavelength. The absorption spectra of sputtered deposited TiO_2 thin films for various sputter power and substrate temperature are shown in Fig. 4(a) and Fig. 4(b). The absorption spectra of TiO_2 thin films shift toward longer wave length. These results show the optical properties of TiO_2 thin films strictly depend upon the sputtered power and substrate temperature. Band gap value can be estimated by the absorption spectra edges[36-39].

The direct optical band gap of sputtered deposited TiO_2 thin films were estimated using tauc's relation[40]:

$$\alpha h\nu = A\left(h\nu - E_g\right)^{1/2}$$

where α is the absorption coefficient, $h\nu$ is the photon energy, E_g the optical band gap of TiO_2 thin films and A is proportional coefficient.

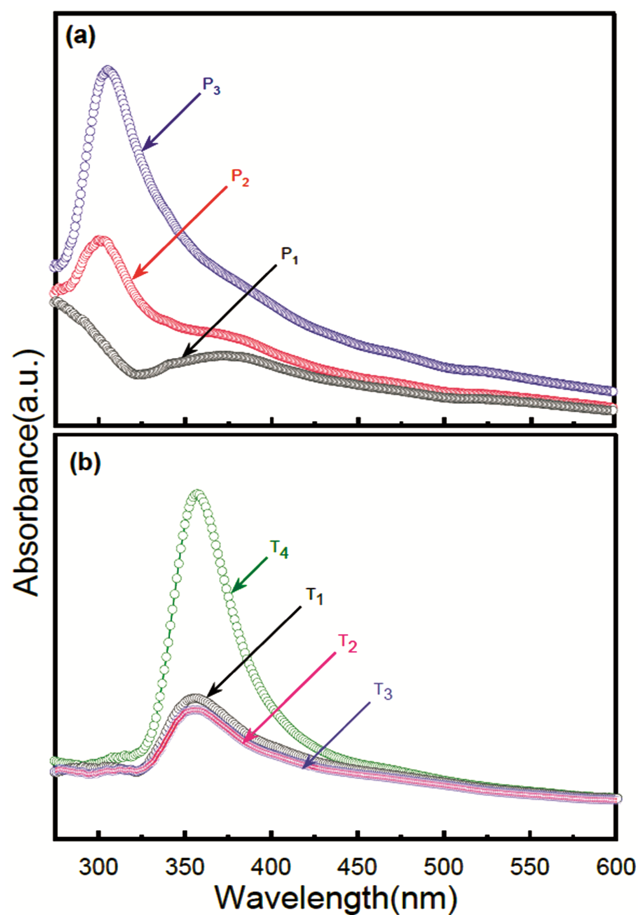

Fig. 4 — Absorption spectra of TiO_2 thin films on glass substrates at: (a) various sputter power, (b) various substrate temperatures.

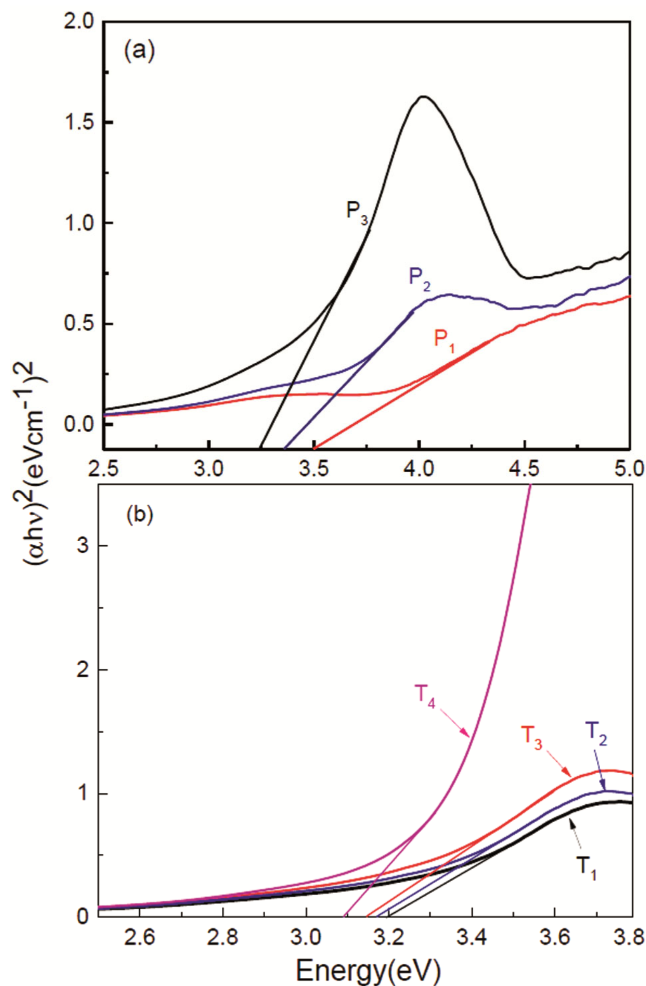

Fig. 5 — Tauc's plot of TiO_2 thin films on glass substrates at: (a) various sputter power and (b) various substrate temperatures.

The Tauc's plot $(\alpha h\upsilon)^2$ versus energy ($h\upsilon$) shown in Fig. 5(a) and Fig. 5(b). The estimated band gap energy values for the samples P_1, P_2 and P_3 are 3.50, 3.35 and 3.25 eV respectively and for the samples T_1, T_2, T_3 and T_4 are 3.25, 3.17, 3.14 and 3.08 eV respectively. As the sputtered power and substrate temperature increases the band gap energy moves from UV to visible region. Narrowing in the optical band gap improves the electronic and optical properties of TiO_2thin films which enhance the photocatalytic activity and antibacterial activity [16,41-42]. By controlling these deposition parameters we can tailored the band gap energy of TiO_2 thin films for various applications.

Conclusion

In the present research work we have successfully deposited TiO_2thin films by DC reactive magnetron sputtering system. In this work, we have studied the effect of sputtered power and substrate temperature on TiO_2 thin films. The XRD patterns of TiO_2 thin films revealed that amorphous and crystalline nature are highly depend on the deposition parameters. We can control the crystalline nature of TiO_2 thin films with sputtering power and substrate temperature. Raman spectroscopy revealed TiO_2thin films are consist both rutile and anatase phase. The anatase phase was not observed in XRD patterns while it was observed in Raman spectroscopy with particular wave number at 144 cm^{-1}(E_g).The anatase phase is more sensitive for photo catalytic activity in comparison of rutile phase by increasing substrate temperature anatase phase can be achieved. UV-Vis. spectroscopy revealed that the band gap decreases as the sputtering power and substrate temperature increases. The optical response of TiO_2thin films move toward visible region from UV region. The sputter power and the substrate temperature are the key parameter for controlling the structural and optical properties of TiO_2 thin films.

References

1 Kalisz M, Grobelny M, Swiniarski M, Mazur M, Wojcieszak D, Zdrojek M, Judek J & Domaradzki J, *Surf Coat Technol*, 290 (2016) 124.
2 Lei Z & Jian-she L, *Trans Nonferrous Met Soc China*, 17 (2007) 772.
3 Keskin A V, Gencten M, Bozar S, Arvas M B, Gunes S & Sahin Y, *Thin Solid Films*, 706 (2020) 1.
4 Tian L, Xing L, Shen X, Li Q, Ge S, Liu B & Jie L, *Atmos Pollut Res*, 11 (2020) 179.
5 Rodriguez D F, Perillo P M & Barrera M P, *Mater Sci Semicond Process*, 71 (2017) 427.
6 Murugan R & Ram C G, *Mater Today: Proc*, 5 (2018) 415.
7 Bindra P & Hazra A, *Sens & Actuators: B Chem*, 290 (2019) 684.
8 Peeters H, Keulemans M, Nuyts G, Vanmeert F, Lic C, Minjauw M, Detavernier C, Bals S, Lenaerts S & Verbruggen S W, *Appl Catal B: Environ*, 267 (2020) 1.
9 Gurakara S, Ot H, Horzum S & Serin T, *Mater Sci & Eng* B, 262 (2020) 1.
10 Serio S, Jorge M E M, Maneira M J P & Nunes Y, *Mater Chem Phys*, 126 (2011) 73.
11 Shen H, Mi L, Xu P, Shen W & Wang P N, *Appl Surface Sci*, 253 (2007) 7024.
12 Garlisi C, Scandura G Szlachetko J, Ahmadi S, Sa J & Palmisano G, *Appl Catal A: Gen*, 526 (2016) 191.
13 Perez E, Torres M F, Morales G, Murgia V & Shama E, *Procedia Mater Sci*, 8 (2015) 649 .
14 Shanthi J, Aishwarya S & Swathi R, *Chem Data Collect*, 29 (2020) 1.
15 Li G , Zou B, Feng S, Shi H, Liao K, Wang Y, Wang W & Zhang G, *Physica B*, 588 (2020) 1.
16 Komaraiah D, Radha E, Sivakumar J, Reddy M V R & Sayanna R, *Surf Interfaces*, 17 (2019) 1.
17 Jia C L, Wei Z N & Zhou R, Nucl Instrum Methods Phys Res B, 313 (2013) 50.
18 Chang Y Y, Shieh Y N & Kao H Y, *Thin Solid Films*, 519 (2011) 6935.
19 Chen T, Luo C, Wang D & Xiong Y, *Phys Procedia*, 18 (2011) 136.
20 Twu M J, Chiou A H, Hu C C, Hsu C Y & Kuo C G, *Polym Degrad Stabil*, 117 (2015) 1.
21 Sharma H K, Sharma S K, Kumar S & Singh B P, *Indian J of Pure Appl Phys*, 58 (2020) 825.
22 Zhao Y X, Han S, Lin Y, Hu C H, Hua L Y, Lee C, Hung Y C & Weng K W, *Surf Coat Technol*, 320 (2017) 630.
23 Barkhade T & Banerjee I, *Mater Today: Proc*, 18 (2019) 1204.
24 Firdausa C M, Rizamb M S B S, Rusopa M & Hidayahc S R, *Procedia Eng*, 41 (2012) 1367.
25 Pansila P, Witit-anun N & Chaiyakun S, *Procedia Eng*, 32 (2012) 862.
26 Horprathum M, Eiamchai P, Chindaudom P, Pokaipisit A & Limsuwan P, *Procedia Eng*, 32 (2012) 676.
27 Astinchapa B, Moradian R & Gholami K, *Mater Sci Semicond Process*, 63 (2017) 169.
28 Lin C P, Chen H, Nakaruk A, Koshy P & Sorrell C C, *Energy Procedia*, 34 (2013) 627.
29 Mazur M, *Opt Mater*, 69 (2017) 96.
30 Zheng S K, Wang T M, Wang C & Xiang G, *Nucl Instrum Methods Phys Res B*, 187 (2002) 479.
31 Frank O, Zukalova M, Laskova B, Kurti J, Koltai J & Kavan L, *Phys Chem Chem Phys*, 14 (2012) 14567.
32 Ma H L, Yang J Y, Dai Y, Zhang Y B, Lu B & Ma G H, *Appl Surf Sci*, 253 (2007) 7497.
33 Surmacki J, Wronski P, Nicze M S & Abramczyk H, *Chem Phys Lett*, 566 (2013) 54.
34 Hardcastle F D, Ishihara H, Sharma R & Biris A S, *J Mater Chem*, 21 (2011) 6337.
35 Nezar S, Saoula N, Sali S, Faiz M, Mekki M, Laoufi N A & Tabet N, *Appl Surf Sci*, 395 (2017) 172.
36 Hasan N B, Haider A J & Amar M A A, *Europ J Sci Res*, 69 (2012) 520.
37 Nair P B, Justinvictor V B, Daniel G P, Joy K, Ramakrishnan V, Kumar D D & Thomas P V, *Thin Solid Films*, 550 (2014) 121.
38 Mekprasart W, Khumtong T, Rattanarak J, Techitdheera W & Pecharapa W, *Energy Procedia*, 34 (2013) 746 .
39 Horprathuma M, Eiamchaia P, Chindaudoma P, Pokaipisitb A & Limsuwan P, *Procedia Eng*, 32 (2012) 676.
40 Gaur J, Sharma H K, Sharma S K & Singh B P, *Indian J of Pure Appl Phys*, 57 (2019) 709.
41 Ghicov A, Macak J M, Tsuchiya H, Kunze J, Haeublein V, Kleber S & Schmuki P, *Chem Phys Lett*, 419 (2006) 426.
42 Sharma H K, Sharma S K, Vemula K, Koirala A R, Yadav H M & Singh B P, *Solid State Sci* , 112 (2021) 1.
43 Wategaonkar S B, Pawar R P, Parale V G, Nade D P, Sargar B M & Mane R K, *Mater Today: Proc*, 23 (2020) 444.
44 Singh K J, Sahni M & Rajoriya M, *Mater Today: Proc*, 12 (2019) 565.